The Sea-Breeze Forerunner

J. E. GEISLER AND F. P. BRETHERTON[1]

Institute of Atmospheric Science, University of Miami, Coral Gables, Fla.

(Manuscript received 5 July 1968, in revised form 10 October 1968)

ABSTRACT

The response of a stably stratified atmosphere to differential heating across a coastline is studied. A linear, inviscid, Boussinesq theory is used to analyze the growth caused by switching on a small temperature contrast at an initial time. The propagation of the disturbance is interpreted in terms of internal gravity waves. The outer part of the disturbance, where the linearization is always valid, arrives ahead of the main nonlinear overturning, the sea breeze proper, and can therefore be described as the sea-breeze forerunner. Solutions are obtained and discussed for three different assumed model atmospheres, illustrating the influence of thermal stratification upon the structure of the forerunner. Some modifications are introduced to enable the effects of viscosity to be described. Reasonable values of internal viscosity and of surface drag are inserted into the modified theory, and these effects, respectively, are found to limit the amplitude of the forerunner at moderate distances inland to a few meters per second and to limit the inland penetration distance to about 60 km.

Implications of the results of this study for a more general nonlinear theory are emphasized. In particular, the role of the upper boundary condition in a model of the sea-breeze circulation is clarified. The momentum balance argument advanced here should also be valid in the nonlinear case.

1. Introduction

The sea breeze is air moving inland from over the sea in response to differential heating across the coastline. The zone which separates this air from that over the land is frequently observed to be so narrow as to take on the character of a *sea-breeze front*. A weak return flow is found in a deep layer above the sea breeze, and the *sea-breeze circulation* is closed by gradual subsidence in the region behind the frontal zone extending out to sea. A more detailed discussion of the observed aspects of the sea-breeze circulation with references to published literature on the subject is to be found in a recent review article by Schroeder *et al.* (1967).

The differential thermal structure which drives the sea-breeze circulation is created by heat put in at the ground and distributed aloft by turbulent diffusion. A definitive feature of the circulation which develops in response to this thermal contrast is that it is thoroughly nonlinear. The flooding of the land with sea air modifies the thermal pattern which initiated the response. The altitude range over which the heat is diffused before the sea breeze begins, and at later times ahead of the sea-breeze front, is likely to be of consequence to the further evolution of the circulation. The rate of growth of the circulation may be appreciably slowed or even brought to a stop by surface drag. If there is synoptic-scale motion of the atmosphere in which the sea breeze is imbedded, the differential heating pattern will be altered; and advection of momentum may modify the circulation. Similarly, synoptic-scale features of stable stratification may be sufficiently strong to limit the altitude range over which heat is diffused, and these features can also be expected to effect dynamical modification of the circulation.

Nonlinear numerical models of the sea-breeze circulation have been advanced by Pearce (1955), Fisher (1961) and Estoque (1961, 1962). The models of Pearce and of Fisher duplicate some of the observed features of the circulation, including a return flow weaker than the inflow and distributed through a deeper layer, the rate of development of the circulation, and the deviation of wind direction due to Coriolis force. Estoque (1961) developed a model of the sea-breeze circulation which differs from these in allowing the turbulent diffusion of heat and momentum to be dependent upon the local velocity and temperature fields. An interesting feature resembling the sea-breeze front was found to develop in this model. The model was then used (Estoque, 1962) to investigate the effect of synoptic-scale flow on the evolution of the sea-breeze circulation. The feature resembling the sea-breeze front failed to develop when the synoptic-scale flow was directed from sea to land, and it failed to develop in the single case where a large stable stratification was imposed.

If the physics of the sea-breeze circulation is to be understood by numerical modeling, then such models will have to be extended to cover a much wider range of external conditions. What is required is the definition of particular types of sea-breeze circulations and their identification with a particular set of governing circumstances. The problem at present is that we do not have sufficient understanding to be able to predict from a

[1] On leave from Kings College, Cambridge University, England.

given set of synoptic-scale conditions where and when the sea-breeze front will develop, how far and how fast it may penetrate inland, or even whether it is meaningful to speak at all times of a sea-breeze front.

The problem may be stated in more general terms by saying that we do not have sufficient understanding of how the atmosphere responds to differential heating on the space and time scales responsible for the sea breeze. It is the object of this paper to attack this problem from a different viewpoint, investigating the response within the framework of an analytic theory. Though not capable of treating the sea-breeze circulation in its entirety, this linear theory does describe one aspect of the response that should appear in both the atmosphere and in a nonlinear numerical model. This is a disturbance which is generated at the coast and propagates both inland and out to sea. On land it produces a wind from the direction of the sea, but this is local air and not air advected in from the sea. Except in the very near vicinity of the coast, it should be felt prior to the arrival of the main nonlinear overturning which is the sea breeze proper. For this reason it has been termed the *sea-breeze forerunner*.

Within the context of the linear theory, the sea-breeze forerunner has a unique interpretation as a superposition of propagating, internal gravity wave modes. Its existence can be attributed to an intrinsic signal velocity in the atmosphere—the group velocity of an internal gravity wave mode—which communicates to an inland point the information that there is a disturbance at the coast. At the inland point the larger scale modes arrive first. With the passage of time, progressively smaller scale modes arrive until singularities begin to build up and the linearization becomes invalid. In this paper the disturbance is generated by switching on a temperature perturbation through a layer of finite depth over the land. Solutions which describe the subsequent development of the disturbance in the absence of friction and heat diffusion are obtained and interpreted. Particular attention is given to assessing the influence of the large-scale stratification. The modifications due to viscosity are considered and the momentum balance is analyzed.

Some of the physical insight obtained in this investigation may prove useful in understanding the behavior of the sea-breeze circulation and nonlinear models which seek to describe it. In particular, the role of stratification in concentrating the disturbance is illuminating and has implications for the choice of an upper boundary condition in a numerical model. The analysis here differs from that of a linear model of the sea breeze, such as that of Haurwitz (1959), in that it considers the initial development for a few hours after a sharp onset of the thermal contrast. For simplicity, the Coriolis force is neglected and no motion occurs on a synoptic scale.

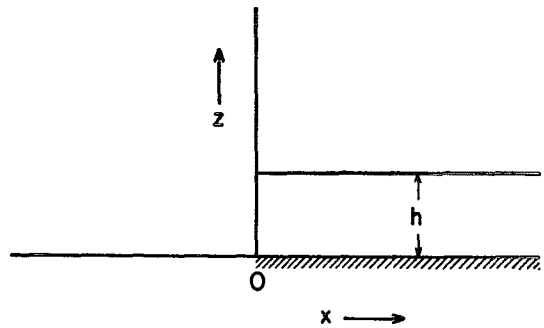

FIG. 1. The coordinate system used, with x positive inland. Heating over the land is assumed to be confined to a layer of depth h.

2. Formulation of the problem

An initially static atmosphere is heated differentially across an infinitely long coastline perpendicular to the x, z plane (Fig. 1). All of the heat is put in at the initial time $t=0$, producing an increase of potential temperature by amount θ_0' in a layer $0\leq z<h$ over the land. The atmosphere is considered to be a Boussinesq incompressible fluid. As will be seen, appreciable motions are confined to a depth which is very much less than the scale of density variation in the vertical and the use of the Boussinesq approximation therefore gives a consistent result. The linearized momentum equations and continuity equation are then

$$\frac{\partial u}{\partial t}=-(1/\bar{\rho}_m)\frac{\partial}{\partial x}p', \tag{1}$$

$$\frac{\partial w}{\partial t}=-(1/\bar{\rho}_m)\frac{\partial}{\partial z}p'-\rho' g, \tag{2}$$

$$\frac{\partial u}{\partial x}+\frac{\partial w}{\partial z}=0, \tag{3}$$

where the velocity components are of perturbation magnitude, $\bar{\rho}_m$ is a mean reference density, and p' and ρ' are perturbation pressure and density. The linearized thermodynamic equation may be written in the form

$$\frac{\partial}{\partial t}\sigma'+N^2w=g(\theta_0'/\bar{\theta}_m)\delta(t)H(x)H(h-z). \tag{4}$$

Here $N^2=(g/\bar{\theta}_m)d\bar{\theta}/dz$ is the Brunt-Vaisala frequency, $\bar{\theta}(z)$ the basic-state potential temperature and

$$\sigma'=-g\rho'/\bar{\rho}_m=g\theta'/\bar{\theta}_m \tag{5}$$

is the buoyancy force. The right-hand side of (4) is the forcing provided by the initial potential temperature perturbation, $\delta(t)$ is a delta function, and $H(x)$ and $H(h-z)$ are Heaviside unit functions.

The continuity equation permits the definition of a stream function

$$u=\frac{\partial\psi}{\partial z},\quad w=-\frac{\partial\psi}{\partial x}. \tag{6}$$

Substitution of the stream function into (1) and (2), followed by cross-differentiation to eliminate the pressure leads to a vorticity equation of the form

$$\frac{\partial}{\partial t}\left(\frac{\partial^2\psi}{\partial x^2}+\frac{\partial^2\psi}{\partial z^2}\right)+\frac{\partial\sigma'}{\partial x}=0. \tag{7}$$

This equation describes the response of the fluid to a horizontal temperature gradient and states that potential temperature increasing in the positive x direction will decrease the local vorticity, taken positive clockwise looking into the plane of Fig. 1. After the initial instant the field of potential temperature is modified only by advection of the basic-state potential temperature, as described by (4).

Except in a region very close to the coast, it turns out that the horizontal scale of vertical motion is very much larger than the vertical scale of horizontal motion, i.e., $\partial^2\psi/\partial x^2\ll\partial^2\psi/\partial z^2$, and therefore may be omitted in (7). This corresponds to the omission of the term $\partial w/\partial t$ in (2), leaving the hydrostatic equation. Alternatively, this result may be anticipated by viewing the disturbance at any time as a superposition of plane internal gravity waves. It is a property of the non-hydrostatic modes that the group velocity vector makes an appreciable angle with the horizontal and the influence of these modes will not be felt very far inland (see Bretherton, 1967).

Eqs. (4) and (7) may then be combined to give

$$\frac{\partial^2}{\partial t^2}\left(\frac{\partial^2\psi}{\partial z^2}\right)+N^2\frac{\partial^2\psi}{\partial x^2}=-g(\theta_0'/\bar{\theta}_m)\delta(t)\delta(x)H(h-z), \tag{8}$$

which describes the evolution of a field of motion excited by the temperature perturbation θ_0' switched on discontinuously at $t=0$. It is to be solved subject to the initial conditions

$$\psi=\frac{\partial\psi}{\partial t}=0,\quad \text{at}\quad t=0, \tag{9}$$

and the boundary conditions

$$\psi=0,\quad \text{on}\quad z=0\quad\text{and}\quad D=0. \tag{10}$$

The upper boundary condition corresponds to a rigid lid imposed at $z=D$ and is discussed in the next section.

3. Method of solution

The homogeneous form of Eq. (8) has solutions of the form

$$\psi=\mathrm{Re}[A\exp\{i(kx+mz-\omega t)\}].$$

These are plane internal gravity waves having a dispersion relation $\omega^2=k^2N^2/m^2$. For given m, their propagation in the horizontal direction is nondispersive, the phase and group velocity both being equal to N/m. Eq. (8) is linear and any solution may be constructed as a superposition of these internal gravity wave modes. If the initial field of ψ excited by the forcing on the right-hand side of the equation is thought of as a superposition of internal gravity wave modes, the solution at a point a distance $|x|$ from the coast at time t will be the superposition of all the modes which have propagated this distance or further in the elapsed time.

The method adopted for the solution of (8) follows very closely this description of the disturbance as a superposition of propagating gravity waves. In its bare essentials, the method consists of placing a rigid lid at height D and expanding the heating function and the solution in terms of a set of orthogonal functions defined on the interval $0\leq z\leq D$. This procedure leads to a separation of variables in (8). In the final summation over the products of the separation variables, the rigid lid is allowed to recede to infinity and the summation is replaced by an integral.

The heating function is expanded in a set of orthogonal functions $\bar{\psi}_n(z)$ according to

$$g(\theta_0'/\bar{\theta}_m)H(h-z)=N^2(z)\sum_{n=1}^{\infty}A_n(z)\bar{\psi}_n(z), \tag{11}$$

where the coefficients are given by

$$A_n(z)=g(\theta_0'/\bar{\theta}_m)\int_0^h\bar{\psi}_n(z)dz\left[\int_0^D N^2(z)[\bar{\psi}_n(z)]^2dz\right]^{-1}. \tag{12}$$

Solutions of (8) are then sought in the form

$$\psi(x,z,t)=\sum_{n=1}^{\infty}f_n(x,t)\bar{\psi}_n(z). \tag{13}$$

Substitution from (11) and (13) into (8) leads to equations defining $f_n(x,t)$ and $\bar{\psi}_n(z)$ in terms of a separation constant $(c_n)^{-2}$, i.e.,

$$-\frac{1}{c_n^2}\frac{\partial^2}{\partial t^2}f_n+\frac{\partial^2}{\partial x^2}f_n=-\delta(t)\delta(x)A_n, \tag{14}$$

$$\frac{\partial^2}{\partial z^2}\bar{\psi}_n+\frac{N^2}{c_n^2}\bar{\psi}_n=0. \tag{15}$$

The modal structure of the solution is now apparent. Internal gravity wave modes excited at the coast ($x=0$) have a vertical structure given by the solution of (15) with boundary conditions $\bar{\psi}_n=0$ on $z=0$ and $z=D$. Each mode travels to the right and to the left with the appropriate phase speed of magnitude c_n, equal also to the horizontal component of group velocity. The

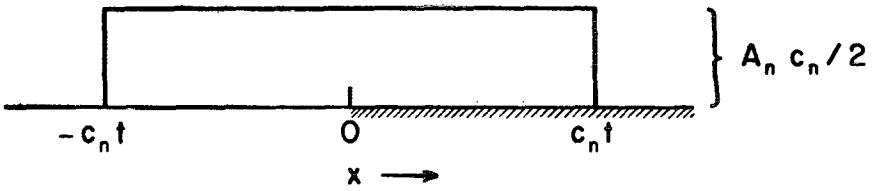

FIG. 2. The function $f_n(x,t)$ vs distance from the coast ($x=0$).

solution of (14), subject to the initial conditions $f_n=\partial f_n/\partial t=0$ at $t=0$ is

$$f_n(x,t)=(A_nc_n/2)[H(x+c_nt)-H(x-c_nt)], \quad (16)$$

where H is the Heaviside unit function. This solution is displayed graphically in Fig. 2. It corresponds to a pulse propagating inland and out to sea with speed c_n. The behavior of this function is an expression of the fact that a particular mode excited at the coast contributes to the superposition a distance $|x|$ from the coast at time t only if the phase velocity of that mode satisfies the condition $|x|t^{-1}\leq c_n$.

The details of the stratification of the atmosphere are assigned by the form of $\bar{\theta}(z)$ and are reflected in the vertical structure of the eigenfunctions defined by (15). Each new case treated requires a solution of the vertical structure equation, but the form of f_n remains the same. The relative amount of forcing that goes into a particular mode comes into the formulation by way of the coefficients A_n.

In the final superposition the rigid lid is assumed to be at an infinite height above the ground, giving a continuum of eigenfunctions and allowing the summation to be replaced by an integral; thus

$$\psi(x,z,t)=\sum_{n=1}^{\infty} f_n(x,t)\bar{\psi}_n(z)$$
$$=\frac{1}{\Delta(1/c_n)}\int_0^{\infty} f(x,t,c)\bar{\psi}(z,c)d\left(\frac{1}{c}\right). \quad (17)$$

The fact that a solution is obtained in which the motion is confined to a region near the ground and is independent of D when D is large shows that the rigid lid is physically unneccessary. Except for the case when N^2 is independent of altitude, the eigenvalues c_n are not easily found. In practice, a knowledge of the eigenvalues is not required, since only the *spacing* $\Delta(1/c_n)$ between eigenvalues enters (17).

4. Results

a. *Model with N^2 independent of altitude (Model I)*

In this case, $\bar{\theta}(z)$ is a linear function of altitude. Over the land the potential temperature in a layer of depth h is $\bar{\theta}(z)+\theta_0'$ at the initial time. The eigenfunctions defined by (15) in this case are

$$\bar{\psi}_n=\sin(Nz/c_n), \quad (18)$$

the eigenvalues c_n being determined by the condition that $\bar{\psi}_n=0$ on $z=D$, leading to the spacing

$$\Delta(1/c_n)=\pi/ND. \quad (19)$$

For this set of eigenfunctions, the coefficients defined by (12) become

$$A_n=2g(\theta_0'/\bar{\theta}_m)(c_n/N^3D)[1-\cos(Nh/c_n)], \quad (20)$$

and substitution of this expression for A_n into (16) leads to

$$f_n=g(\theta_0'/\bar{\theta}_m)(c_n^2/N^3D)\{1-\cos(Nh/c_n)\}$$
$$\times[H(x+c_nt)-H(x-c_nt)]. \quad (21)$$

The superposition equation (17) may now be evaluated from (18), (19) and (21) to give the solution in the form

$$\psi(x,z,t)=\frac{g(\theta_0'/\bar{\theta}_m)}{\pi N^2}\int_0^{\infty}\sin(Nz/c)\{1-\cos(Nh/c)\}$$
$$\times[H(x+ct)-H(x-ct)]c^2d\left(\frac{1}{c}\right). \quad (22)$$

The height D of the rigid lid, appearing in (19) and (21), does not enter the final expression.

The quantity Nc^{-1} which appears in (22) may be identified from (15) as the vertical wavenumber of a given mode. The integral in (22) is thus over all vertical wavenumbers. The function in the square brackets is unity when c satisfies the condition $|x|t^{-1}\leq c$ and zero otherwise (see Fig. 2.) In terms of the dimensionless variable of integration $\eta=Nh/c$, where h is the depth of the heated layer, the effect of this function is to replace the upper limit of integration by the finite quantity

$$\tau=Nht/|x|; \quad (23)$$

it therefore behaves as a filter, admitting modes with wavenumbers less than a cutoff value. Differentiation of (22) with respect to z gives an expression for the horizontal velocity. In terms of the new variables η and τ, this is

$$u(x,z,t)=\frac{\partial\psi}{\partial z}=\frac{g(\theta_0'/\bar{\theta}_m)}{\pi N}$$
$$\times\int_0^{\tau}[1-\cos\eta]\cos(\eta z/h)\frac{d\eta}{\eta}. \quad (24)$$

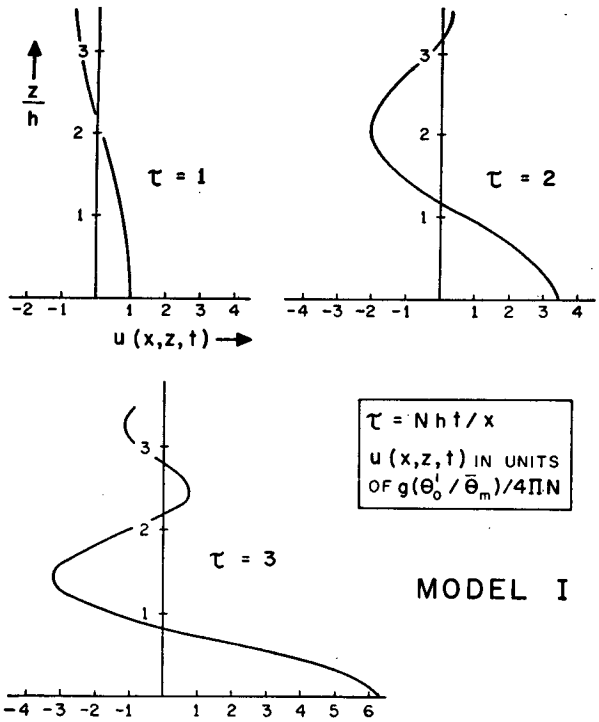

FIG. 3. Evolution of the sea-breeze forerunner in an atmosphere having the structure specified by Model I. Horizontal wind $u(x,z,t)$ is in units proportional to the thermal contrast applied across the coastline through a depth h of the atmosphere at time $t=0$. See Section 4a for numerical values of parameters.

The integral in this expression has been evaluated numerically, results for moderate values of the variable τ being shown in Fig. 3. For a fixed value of distance x inland the figure illustrates the horizontal wind field at successive times. The characteristic feature of the disturbance is that it settles toward the ground as time progresses. At values of τ very much larger than shown here, the inward flow is concentrated near the ground and the return flow is largest at $z=h$, dropping rapidly to zero above this level. The disturbance at large values of τ is, however, dominated by very small scale modes for which the linearization is certainly not valid.

For typical values of the parameters entering (24), we shall take $N=10^{-2}$ sec^{-1}, $h=1$ km, $\theta_0'=2$C. The value of h chosen here applies at the time of the maximum vertical extent of the heated layer, a point which is further considered in Section 7. Then the ordinate in Fig. 3 is altitude in km, while two units on the abscissa scale correspond to about 1 m sec^{-1}. With these values of N and h and at a distance 20 km inland, the unit of τ corresponds to about one-half hour in time. The sequence in Fig. 3 then illustrates the wind to be experienced a distance of 20 km inland at times 0.5, 1.0 and 1.5 hr after the temperature perturbation has been switched on. Insofar as this disturbance provides a significant wind in advance of the arrival of the main nonlinear overturning, the sea breeze proper, it constitutes the sea-breeze forerunner.

b. Two-layer model (Model II)

In this model $\bar{\theta}$ is independent of altitude in the layer $0\leq z<h$ and increases linearly with altitude above $z=h$. This would correspond to an air mass possessing a well-mixed lower layer over both land and sea, with heat supplied to this layer over the land. To treat this case analytically, it is necessary to assume that $\bar{\theta}$ has some slight altitude dependence in the lower layer so that equations can be formulated with a nonzero $N=N_1$ there. In the final stages N_1 will be allowed to become arbitrarily small.

The eigenfunctions in the lower and upper layers are, respectively,

$$\left.\begin{aligned}(\bar{\psi}_1)_n&=\sin(N_1z/c_n)\\ \bar{\psi}_n&=\sin(N_1h/c_n)\sin[N(z-D)/c_n]\\ &\quad\times\{\sin[N(h-D)/c_n]\}^{-1}\end{aligned}\right\}. \tag{25}$$

The eigenvalues are determined by the condition that $\partial\bar{\psi}_n/\partial z$ be continuous across $z=h$, which leads to the relation

$$N\cot[N(h-D)/c_n]=N_1\cot(N_1h/c_n). \tag{26}$$

We are interested in this problem only in the spacing of the eigenvalues and, in this particular case, only when N_1 is small and D large. Specifically, we shall assume that $N_1h/c_n\ll1$ and that $D\gg h$. Then a simple iterative procedure shows that the roots of (26) are separated by an interval

$$\Delta(Nh/c_n)=\pi h/(D-h)+O[h^2/(D-h)^2]. \tag{27}$$

Thus, when $D/h\gg1$, the eigenvalues are spaced as in Model I, that is, as given by (19).

Substitution of the expressions for the eigenfunctions in the upper and lower layer into (12) gives

$$A_n\approx g(\theta_0'/\bar{\theta}_m)\left(\frac{h}{DN_1N}\right)\left(\frac{Nh}{c_n}\right)\times\left[1+\left(1-\frac{h}{D}\right)\left(\frac{Nh}{c_n}\right)^2\right]^{-1}, \tag{28}$$

when the condition $N_1h/c_n\ll1$ is imposed. Under this condition and when (26) is used to eliminate D, Eqs. (25) for the eigenfunctions take the form

$$\left.\begin{aligned}(\bar{\psi}_1)_n&\approx N_1z/h\\ \bar{\psi}_n&\approx(N_1/N)\{\sin[N(z-h)/c_n]\\ &\quad+(Nh/c_n)\cos[N(z-h)/c_n]\}\end{aligned}\right\}. \tag{29}$$

Using Eqs. (27)–(29), we may effect the superposition according to (17). Differentiation with respect to z gives for the horizontal wind in the lower and upper layers,

respectively,

$$\left.\begin{aligned} u(x,t)&=\frac{g(\theta_0'/\bar{\theta}_m)}{2\pi N}\int_0^\tau \frac{\eta}{1+\eta^2}d\eta \\ &=\frac{g(\theta_0'/\bar{\theta}_m)}{4\pi N}\log(1+\tau^2) \\ u(x,z,t)&=\frac{g(\theta_0'/\bar{\theta}_m)}{2\pi N}\left\{\int_0^\tau \frac{\eta}{1+\eta^2}\cos[\eta(z-h)/h]d\eta \right. \\ &\left. -\int_0^\tau \frac{\eta^2}{1+\eta^2}\sin[\eta(z-h)/h]d\eta\right\} \end{aligned}\right\}. \quad (30)$$

The integrals in the expression for the upper layer must again be evaluated numerically.

The results for this model are illustrated in Fig. 4. As time progresses at a fixed distance inland, the disturbance in the upper layer settles to occupy a region closer to $z=h$. The disturbance is independent of altitude in the lower layer at all times. This is a consequence of the fact that $\bar{\theta}$ is independent of altitude in the lower layer; vertical motions cannot then alter the temperature distribution there and on a linear theory the horizontal gradient retains a delta function character at $x=0$ for all time. For the typical values of parameters assumed in the discussion of Model I, the wind in Fig. 4 is again in units of 0.5 m sec^{-1}, approximately, the altitude is in km and successive values of τ are time in units of one-half hour after the temperature perturbation is switched on.

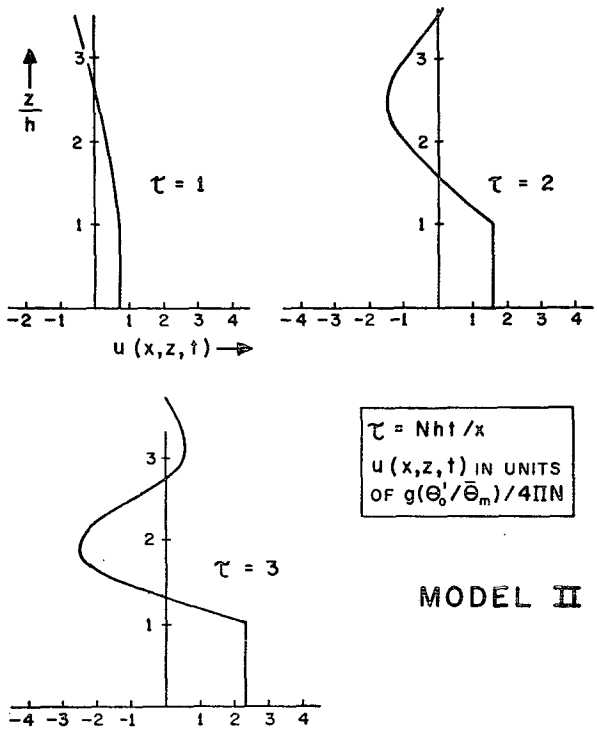

FIG. 4. Same as Fig. 3 but for Model II.

c. Two-layer model with inversion (Model III)

For this model, the temperature distribution in Model II is modified by the introduction of a discontinuity $\Delta\bar{\theta}$ in the basic-state potential temperature at the level $z=h$. This simulates the presence of a sharp inversion capping the well-mixed layer. The eigenfunctions are as given before by Eqs. (25), but the matching condition is now that $\partial\bar{\psi}_n/\partial z$ must jump by an amount

$$\Delta\left(\frac{\partial}{\partial z}\bar{\psi}_n\right)=-g(\Delta\bar{\theta}/\bar{\theta}_m)\bar{\psi}_n/{c_n}^2$$

in passing upward through the level $z=h$. The equation determining the eigenvalues is then

$$N\cot[N(h-D)/c_n]=N_1\cot(N_1h/c_n) -g(\Delta\bar{\theta}/\bar{\theta}_m)/c_n. \quad (31)$$

Again, a simple iterative procedure can be applied to determine the spacing of the roots of this equation and, provided $N_1h/c_n\ll 1$ and $D\gg h$, this is found still to be given by (19).

The only formal difference between the present model and the model without a temperature discontinuity (Model II) appears in the expression for A_n which, for the present case with $N_1h/c_n\ll 1$ and $D\gg h$, is

$$A_n\approx g(\theta_0'/\bar{\theta}_m)\left(\frac{h}{DN_1N}\right)\left(\frac{Nh}{c_n}\right)\left\{1+\left(\frac{Nh}{c_n}\right)^2 \times\left[1-2g\frac{(\Delta\bar{\theta}/\bar{\theta}_m)}{N^2h}\right]+\left(\frac{Nh}{c_n}\right)^4\left[\frac{g(\Delta\bar{\theta}/\bar{\theta}_m)}{N^2h}\right]^2\right\}^{-1}. \quad (32)$$

The quantity $g(\Delta\bar{\theta}/\bar{\theta}_m)$ is introduced into this expression when use is made of (31) to eliminate D where it appears in the argument of a trigonometric function.

The fundamental difference in behavior of the solution in the two models may be seen by examining the solution in the lower layer. In the present model, Eq. (17) differentiated with respect to z gives for the wind in the lower layer

$$u(x,t)=\frac{g(\theta_0'/\bar{\theta}_m)}{2\pi N}\int_0^\tau \frac{\eta}{\eta^2+(1-\alpha^2\eta^2)^2}d\eta, \quad (33)$$

where

$$\alpha=[g(\Delta\bar{\theta}/\bar{\theta}_m)h]^{\frac{1}{2}}(Nh)^{-1}. \quad (34)$$

This may be integrated (when $4\alpha>1$) to give

$$u(x,t)=\frac{g(\theta_0'/\bar{\theta}_m)h}{2\pi N(4\alpha-1)^{\frac{1}{2}}}\left\{\tan^{-1}\left[\frac{2\alpha^2\tau^2-2\alpha+1}{(4\alpha-1)^{\frac{1}{2}}}\right] -\tan^{-1}\left[\frac{1-2\alpha}{(4\alpha-1)^{\frac{1}{2}}}\right]\right\}. \quad (35)$$

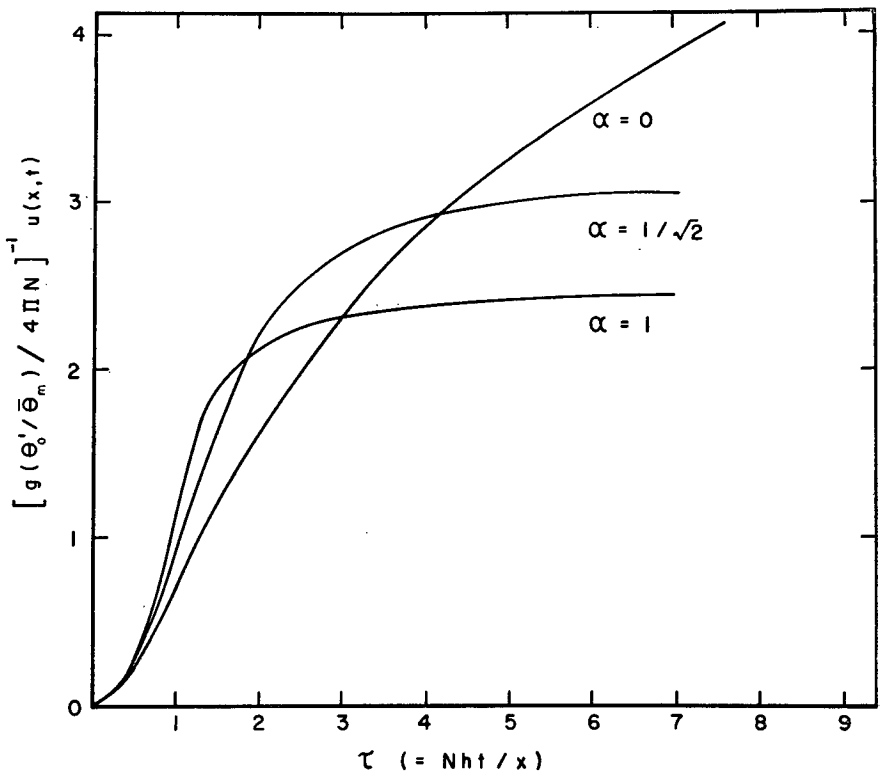

FIG. 5. The rate of increase of the wind in the lower layer at a fixed distance x inland as the forerunner arrives in Model II (curve labeled $\alpha=0$) and in Model III (curves with $\alpha\neq 0$).

The behavior of this solution is illustrated in Fig. 5. When $\alpha=0$, (33) reduces to the first of Eqs. (30) and the curve labeled $\alpha=0$ in Fig. 5 therefore shows the wind in the lower layer in Model II as a function of time at a fixed distance inland. When the temperature discontinuity at $z=h$ is introduced, the wind in the lower layer increases more rapidly with time at first, then approaches a finite steady-state limit.

Alternatively, if time is regarded as fixed, Fig. 5 shows the wind speed in the lower layer as a function of distance inland. The stronger the temperature discontinuity, the more the forerunner takes on the appearance of a surge propagating inland. To understand this feature, it is necessary to consider the limiting case as $\alpha\rightarrow\infty$. For this purpose we write (33) in the form

$$u(x,t)=\frac{g(\theta_0'/\bar{\theta}_m)h}{2\pi[g(\Delta\bar{\theta}/\bar{\theta}_m)h]^{\frac{1}{2}}}\int_0^{\tau^*}\frac{\alpha\eta^*}{\eta^{*2}+\alpha^2(1-\eta^{*2})^2}d\eta^*, \quad (36)$$

where $\eta^*=\alpha\eta$. Calling the integrand $F(\eta^*)$, we note that as $\alpha\rightarrow\infty$, $F(1)\rightarrow\alpha$, while outside an interval of width α^{-1} centered about $\eta^*=1$, $F(\eta^*)\rightarrow 0$. The integrand thus takes on the character of a delta function with argument $(1-\eta^*)$ for large α and, since $\tau^*=\alpha Nht/x$, (36) gives

$$\left.\begin{aligned} u(x,t)&=0, && \text{for } \frac{x}{t}>[g(\Delta\bar{\theta}/\bar{\theta}_m)h]^{\frac{1}{2}} \\ u(x,t)&=\frac{g(\theta_0'/\bar{\theta}_m)h}{2\pi[g(\Delta\bar{\theta}/\bar{\theta}_m)h]^{\frac{1}{2}}}, && \text{for } \frac{x}{t}\leq[g(\Delta\bar{\theta}/\bar{\theta}_m)h]^{\frac{1}{2}} \end{aligned}\right\}. \quad (37)$$

The disturbance at the coast therefore propagates inland and out to sea as a surge with propagation speed $[g(\Delta\bar{\theta}/\bar{\theta}_m)h]^{\frac{1}{2}}$.

5. The effects of viscosity

In the atmosphere the propagation of the sea-breeze forerunner is likely to be significantly modified by the action of eddy viscosity. When the inviscid theory employed thus far is modified to allow for the diffusion of vorticity and a no-slip boundary condition is imposed at the surface, no simple analytic solutions are found. However, it is still possible to gain some insight into the way in which viscosity will act if the effects of internal viscosity are artificially separated from the effects of surface drag.

If a term effecting a diffusion of vorticity is put into Model I of the theory, but the lower boundary condition is allowed to remain as a slip condition, the superposition equation is modified by the appearance of a term

$\exp[-m^3(K|x|/N)]$ inside the integral sign, where K is the eddy diffusion coefficient, assumed independent of altitude, and m the vertical wavenumber of a particular mode. Thus, each mode decays exponentially with distance as it propagates away from the coast. This factor is close to unity for wavenumbers $<(K|x|/N)^{-\frac{1}{3}}$ but is very small for values only slightly greater. The effect of an internal viscosity acting in the absence of surface drag is to introduce at each point a cutoff wavenumber; higher wavenumber modes are damped before reaching the point. The forerunner evolves in the manner detailed in Fig. 3 up to the time that the cutoff mode arrives. This time is given by

$$KN^2t^3/x^2=1,$$

the left-hand side of this equation being the argument of the exponential factor evaluated at the upper limit of integration τ. The cutoff time is independent of the depth of the heated layer and weakly dependent upon the viscosity as $K^{-\frac{1}{3}}$. If we take $N=10^{-2}$ sec^{-1} and $x=20$ km, as earlier, and $K=2\times10^5$ cm^2 sec^{-1}, then $t\approx6000$ sec. The forerunner as presented in Fig. 3 is then largely unmodified at this distance inland but does not develop further beyond $\tau=3$.

To properly assess the effect of viscosity, surface drag must be considered. A crude model of the forerunner which incorporates this can be obtained by modifying Model II to include a drag force uniformly distributed throughout the lower layer. This assumes an eddy viscosity coefficient that is infinite in the lower layer and zero in the upper layer. The problem is kept linear by expressing the stress at the surface in the form

$$\bar{\rho}_m C_D u^2=\bar{\rho}_m(C_D U)u,$$

where C_D is a drag coefficient and U a typical value of wind speed in the lower layer. Some effect is to be expected from the fact that surface drag over the sea is different than that over the land, but this is not considered here.

With this modification, the governing equation becomes

$$\frac{\partial}{\partial t^2}\left(\frac{\partial^2\psi}{\partial z^2}\right)+N^2\frac{\partial^2\psi}{\partial x^2}=-\left[g(\theta_0'/\bar{\theta}_m)\delta(t)\delta(x)+\gamma\frac{\partial}{\partial t}\left(\frac{\partial^2\psi}{\partial z^2}\right)\right]H(h-z), \quad (38)$$

where

$$\gamma=C_D U h^{-1}, \quad (39)$$

and has the dimensions of inverse time. It is convenient at this stage to take the Laplace transform of (38), introducing the transform variable

$$\hat{\psi}(x,z,s)=\int_0^\infty \psi(x,z,t)e^{-st}dt. \quad (40)$$

The resulting equation in the transform variable may be treated by the method outlined in Section 3. The separation constant is now $(s/c_n)^2$ and the solutions of the equations in the separation variables are

$$f_n=A_n\frac{s}{c_n}\exp\left(-\frac{s}{c_n}|x|\right), \quad (41)$$

$$\left.\begin{aligned}(\bar{\psi}_1)_n&=\sin\left[\frac{N_1}{c_n}\left(\frac{s}{\gamma+s}\right)^{\frac{1}{2}}z\right]\\ \bar{\psi}_n&=\sin\left[\frac{N_1}{c_n}\left(\frac{s}{\gamma+s}\right)^{\frac{1}{2}}h\right]\\ &\quad\times\sin[N(z-D)/c_n]/\sin[N(h-D)/c_n]\end{aligned}\right\}. \quad (42)$$

Eqs. (42) for the eigenfunctions in the lower and upper layer, respectively, reduce to Eqs. (25) when $\gamma=0$. The matching condition at $z=h$ is

$$\left(\frac{\gamma+s}{s}\right)\frac{\partial}{\partial z}(\bar{\psi}_1)_n=\frac{\partial}{\partial z}\bar{\psi}_n, \quad (43)$$

leading to the eigenvalue equation

$$N\cot[N(h-D)/c_n]=\left(\frac{\gamma+s}{s}\right)^{\frac{1}{2}}N_1\cot\left[\frac{N_1}{c_n}\left(\frac{s}{\gamma+s}\right)^{\frac{1}{2}}h\right]. \quad (44)$$

When $N_1h/c_n\ll1$ and $D/h\gg1$, the eigenvalues are separated by an interval

$$\Delta(Nhs/c_n)=\pi hs/D. \quad (45)$$

The construction of the solution then proceeds formally as for Model II, resulting in the lower layer equation

$$\hat{u}(x,s)=\frac{1}{2\pi Ns}\int_0^\infty\frac{\eta\exp[-s|x|\eta/(Nh)]}{[(\gamma+s)/s]^2+\eta^2}d\eta. \quad (46)$$

This integral may be evaluated in terms of the cosine and the sine integral functions $\mathrm{Ci}(y)$ and $\mathrm{si}(y)$ to give

$$\hat{u}(x,s)=-\frac{1}{2\pi Ns}[\mathrm{Ci}(y)\cos(y)+\mathrm{si}(y)\sin(y)], \quad (47)$$

where

$$y=(\gamma+s)|x|/(Nh).$$

The complete formal solution is obtained by inversion of the Laplace transform according to

$$u(x,t)=\frac{1}{2\pi i}\int_{-i\infty}^{i\infty}\hat{u}(x,s)e^{st}ds. \quad (48)$$

The function $\hat{u}(x,s)$ has a branch cut along the negative real axis for $|s|\geq\gamma$ and the contour may be deformed into a portion running along either side of the branch cut plus a closed path encircling the origin. Integration

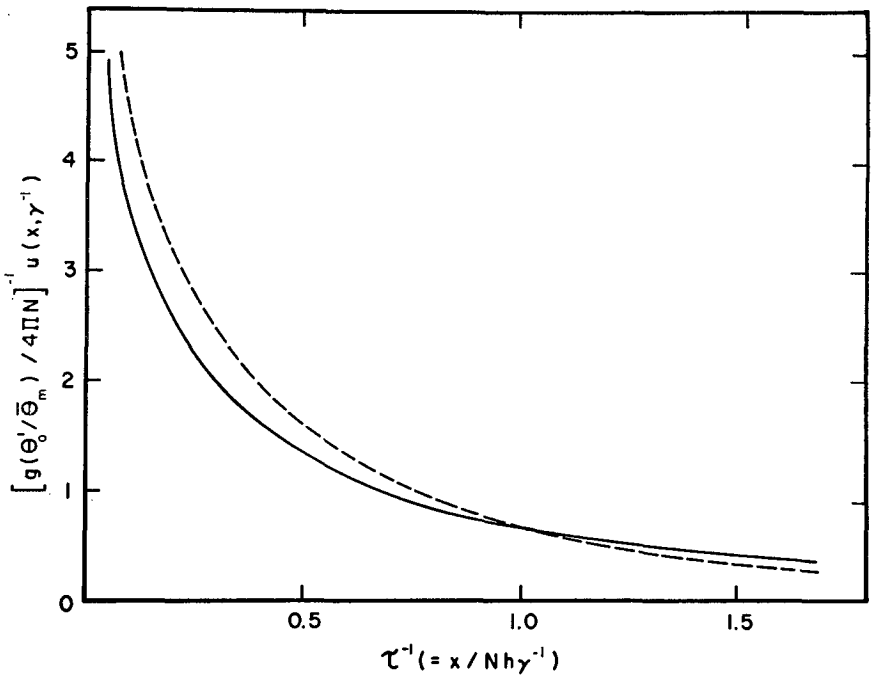

FIG. 6. The wind in the lower layer in Model II vs distance from the coast at time $t=\gamma^{-1}$ is represented by the broken line. The steady-state wind in the lower layer when Model II is modified to include surface drag is represented by the full line.

on the contour running along either side of the branch cut yields the transient solution. The steady-state solution is obtained by integration on the contour around the origin. This gives $2\pi i$ times the residue there and the steady-state solution is then

$$u(x,\gamma)=-\frac{1}{2\pi N}\left[\mathrm{Ci}\left(\frac{\gamma|x|}{Nh}\right)\cos\left(\frac{\gamma|x|}{Nh}\right)+\mathrm{si}\left(\frac{\gamma|x|}{Nh}\right)\sin\left(\frac{\gamma|x|}{Nh}\right)\right]. \quad (49)$$

Fig. 6 shows this steady-state wind in the lower layer plotted on a scale proportional to distance inland. Also shown is $u(x,\gamma^{-1})$ from the first of Eqs. (30) which is the velocity in Model II at the time $t=\gamma^{-1}$. It may be seen that the essential effect of surface drag is to freeze the circulation at its stage of development at time $t=\gamma^{-1}$.

To estimate the time γ^{-1} required to set up the steady-state circulation, we must assign values to the quantities h, C_D and U appearing in (39). Clearly, h must be treated in this context as an average over the time span from dawn until time of maximum vertical extent of the heated layer. We adopt the value $h=500$ m for this calculation. For the drag coefficient C_D we take a value based on a published figure of Sawyer (1959), who has chosen a value of 1.5×10^{-6} for the ratio of surface stress to the square of the geostrophic wind to be representative of conditions over land generally. This figure is based on an assumed value of 0.3 for the ratio of anemometer level wind to geostrophic wind and corresponds to a value $(C_D)_{10}\approx1.7\times10^{-2}$ for the drag coefficient referred to anemometer level. For our estimate we shall assume that the wind in the lower layer, to which the drag coefficient C_D in (39) is referred, is twice the anemometer level wind, so that $C_D=0.25(C_D)_{10}\approx4.3\times10^{-3}$. Then, for an assumed value $U=3$ m sec^{-1} for the typical velocity in the lower layer and $h=500$ m, we arrive at the estimate $\gamma^{-1}\approx10$ hr and a stress $\bar{\rho}_m(C_DU)u$ of about 0.4 dyn cm^{-2} when $u=U$. For this value of γ^{-1} the ordinate in Fig. 6 is distance inland in units of approximately 200 km; the unit of wind speed is as in earlier figures about 0.5 m sec^{-1}. On these considerations, the forerunner can attain a strength of 1 m sec^{-1} some 60 km inland, for example, and is at this stage checked by surface drag. However, the 10 hr required for this is sufficiently long that turning of the wind by the Coriolis force should be just as effective in limiting the penetration distance.

6. Momentum balance

It is instructive to consider which qualitative features of these results follow from quite general considerations.

The horizontal momentum acquired by that part of the fluid enclosed in a box of length $2L$ centered at the coast ($x=0$) and extending to a height z is

$$M=\bar{\rho}_m\int_0^z dz\int_{-L}^{L} u\,dx. \quad (50)$$

Integration of the inviscid horizontal equation of motion (1) leads to

$$\frac{\partial M}{\partial t}=-\int_0^z dz\int_{-L}^{L}\frac{\partial p'}{\partial x}dx$$

$$=-\int_0^z [p'(L,z)-p'(-L,z)]dz, \quad (51)$$

where $p'(x,z)$ is the perturbation pressure, related to the perturbation potential temperature θ' by the hydrostatic equation in the form

$$\frac{\partial p'}{\partial z}=g(\bar{\rho}_m/\bar{\theta}_m)\theta'. \quad (52)$$

Integration of the hydrostatic equation to the height D of the rigid lid followed by substitution of the resulting expression for $p'(x,z)$ into (51) gives

$$\frac{\partial M}{\partial t}=g(\bar{\rho}_m/\bar{\theta}_m)\int_0^z dz\left[\int_z^D \theta'(L,\zeta)d\zeta\right.$$

$$\left.-\int_z^D \theta'(-L,\zeta)d\zeta\right]-[p'(L,D)-p'(-L,D)]z. \quad (53)$$

If the box extends to infinity in both horizontal directions, $\theta'(L,\zeta)-\theta'(-L,\zeta)$ may be replaced by a single function $\Delta\theta(\zeta)$, the temperature contrast between points far inland ahead of the forerunner and far out to sea.

We now consider the momentum M_1 in a layer of depth h chosen such that $\Delta\theta(\zeta)=0$ for $\zeta>h$ and yet h/D is small. Then from (53)

$$\frac{\partial M_1}{\partial t}=g(\bar{\rho}_m/\bar{\theta}_m)\int_0^h z\Delta\theta dz$$

$$-[p'(\infty,D)-p'(-\infty,D)]h. \quad (54)$$

But if the box is extended upwards to $z=D$, the total momentum in it must vanish, from continuity. Hence, also from (53)

$$[p'(\infty,D)-p'(-\infty,D)]D=g(\bar{\rho}_m/\bar{\theta}_m)\int_0^h z\Delta\theta dz. \quad (55)$$

Since $\Delta\theta$ vanishes in $h<z<D$,

$$\frac{\partial M_1}{\partial t}=g(\bar{\rho}_m/\bar{\theta}_m)\left[1-\frac{h}{D}\right]\int_0^h z\Delta\theta dz, \quad (56)$$

and, in the limit as $h/D\to 0$, the pressure on the rigid lid plays no role in the momentum balance in the lower layer $z\leqslant h$.

Eq. (56) shows that in the absence of friction the total momentum in the lower layer must continue to increase linearly with time at a rate which depends only on the difference in temperature between points far inland and far out to sea, independently of the stratification or the details of the velocity structure. This conclusion must also hold in a nonlinear theory, provided there is no vertical advection of momentum through the level $z=h$. Thus, if the sea-breeze circulation were to be limited in horizontal extent, it would have to increase in strength indefinitely. If, on the other hand, there is an upper bound to the wind velocity at each point, the circulation must extend inland at constant velocity. These are extremes and Models I and II are intermediate between them. The latter extreme is realized in Model III as $\alpha\to\infty$.

When surface drag is included in the manner detailed in Section 5, then (53) and hence (56) are modified by the addition of a term γM_1 on the left-hand side, where γ is defined by (39). In the steady state, $\partial M_1/\partial t=0$ and the modified form of (56) then gives for the steady-state momentum in the lower layer

$$M_1=\gamma^{-1}g(\bar{\rho}_m/\bar{\theta}_m)\int_0^h z\Delta\theta dz. \quad (57)$$

This result affords a check on the expression derived in Section 5 for the steady-state velocity in the lower layer. Substitution from (49) for $u(x,\gamma)$ into (50) and integration to $z=h$ gives $M_1=\gamma^{-1}g(\rho_m/\bar{\theta}_m)\theta_0'h^2/2$, in agreement with (57).

In general, even on a nonlinear theory, we must have for a steady state

$$\int_{-\infty}^{\infty}\tau_0 dx=g(\bar{\rho}_m/\bar{\theta}_m)\int_0^h z\Delta\theta dz,$$

where τ_0 is the stress at the ground. This provides a measure of the inland penetration of a steady circulation, such as the one considered in Section 5. If we take $\Delta\theta=2$C through a layer of 500 m depth, then the horizontal integral of the stress at the ground must equal 8×10^6 dyn cm^{-1}. If the average value of this stress is set arbitrarily at 0.4 dyn cm^{-2}—the stress in the example in Section 5 when the wind in the lower layer is 3 m sec^{-1}—then the horizontal extent of the circulation must be 200 km. This is a constraint which must be present also in a nonlinear, numerical model.

Extension of the box to the height $z=D$ gives for the equivalent of (55)

$$[p'(\infty,D)-p'(-\infty,D)]D$$

$$=g(\bar{\rho}_m/\bar{\theta}_m)\int_0^h z\Delta\theta dz-\gamma M_1. \quad (58)$$

Since M_1 increases with time to the steady-state value given by (57) and $\Delta\theta=0$ in $h<z<D$, (58) states that the pressure difference across the ends of the box at the rigid lid decreases with time to zero. This behavior is due to the stress at the ground, which tends to accelerate the fluid in the direction from land to sea. In order to

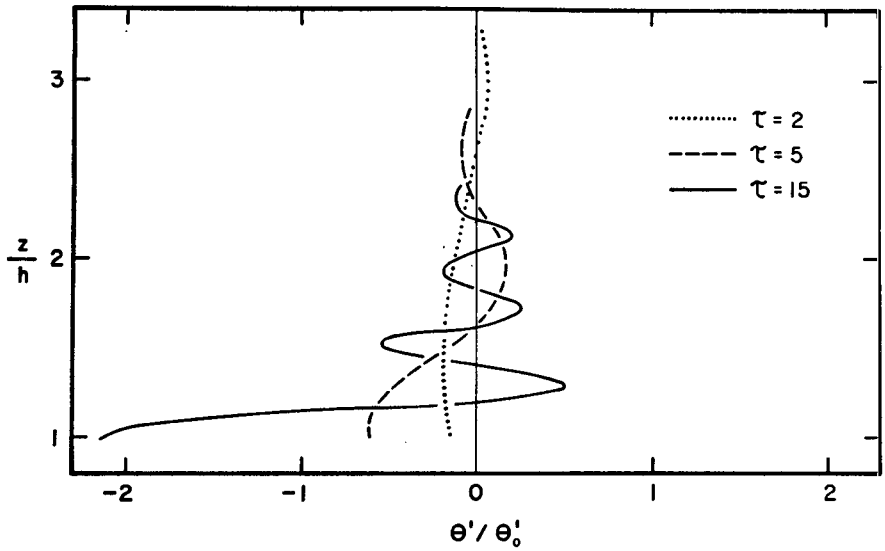

FIG. 7. The perturbation potential temperature θ' over land at successive values of τ(proportional to time) in Model II in units of the lower layer perturbation θ'_0. For overwater conditions, the sign of θ' is reversed.

satisfy the continuity requirement that the momentum M of the fluid in the box extending to $z=D$ be zero, a pressure difference builds up along the rigid lid to oppose this tendency. In the steady state this pressure difference is equal but of opposite sign to the pressure difference set up to drive the return flow at the initial instant.

7. Discussion

The picture that emerges from the linearized inviscid theory in which a thermal contrast is suddenly imposed in the lowest kilometer above land and sea is as follows.

The pressure in the lowest kilometer is systematically lower over land than over sea and there is an accelerating inflow near the earth's surface. Immediately after starting there are no perturbations θ' of potential temperature above this lower layer and the return flow takes place uniformly above it under the influence of a small pressure gradient along and below the rigid lid. However, the vertical velocities associated with the circulation cause a redistribution of potential temperature which tends to concentrate the return flow nearer the ground. The perturbation θ' decreases with time in the upper layer over land and increases over the sea, as illustrated by Fig. 7. There is a net flux of potential temperature from over land to over the sea, because the return flow takes place at higher levels where $\bar{\theta}$ is larger.

The velocity and temperature perturbation at any given point is the superposition of the effects of gravity waves arriving one after the other, each traveling with its appropriate group velocity. The modes with largest vertical scale arrive first; with later arrivals the details of the vertical structure are filled in. For an observer moving inland with any constant velocity, the local structure and magnitude of the perturbation are constant, so that the horizontal extent of the circulation increases indefinitely with time.

If the magnitude of the applied thermal contrast is not infinitesimally small, this theory is not strictly valid. However, nonlinearities are only important for those modes in which the phase velocity is comparable to or smaller than the typical fluid particle velocities. Thus, the computed profiles for large values of τ are unrealistic, but the onset of the forerunner should be adequately described. The essential requirement is that the thermal stratification $\partial\theta/\partial z$ far inland and far out to sea should be approximated by $\partial\bar{\theta}/\partial z$. Then the growth of perturbations θ' which are small compared to $(\partial\bar{\theta}/\partial z)h$ can be described by the linearized theory, although the linearization at any given point will break down after a sufficiently long time.

In all these linearized models, the temperature distribution at the ground is unaltered after the initial heating, because changes in θ' occur only through $w\partial\bar{\theta}/\partial z$ and w vanishes at the ground. Thus, the discontinuity at the origin remains there indefinitely. In practice, however, horizontal advection will always sweep this inland as the sea-breeze front, but at a rate substantially slower than the propagation speed of the onset of the forerunner.

The hydrostatic approximation is normally valid provided the vertical scale of the motion under consideration is small compared to the horizontal scale. In this sense, the step function input into the theory should be regarded as an idealization of a smoothly varying function spread over a horizontal space scale everywhere larger than the vertical scale and over a time scale long compared to the Brunt-Väisälä period. If this smoothness were violated, the only effect would be

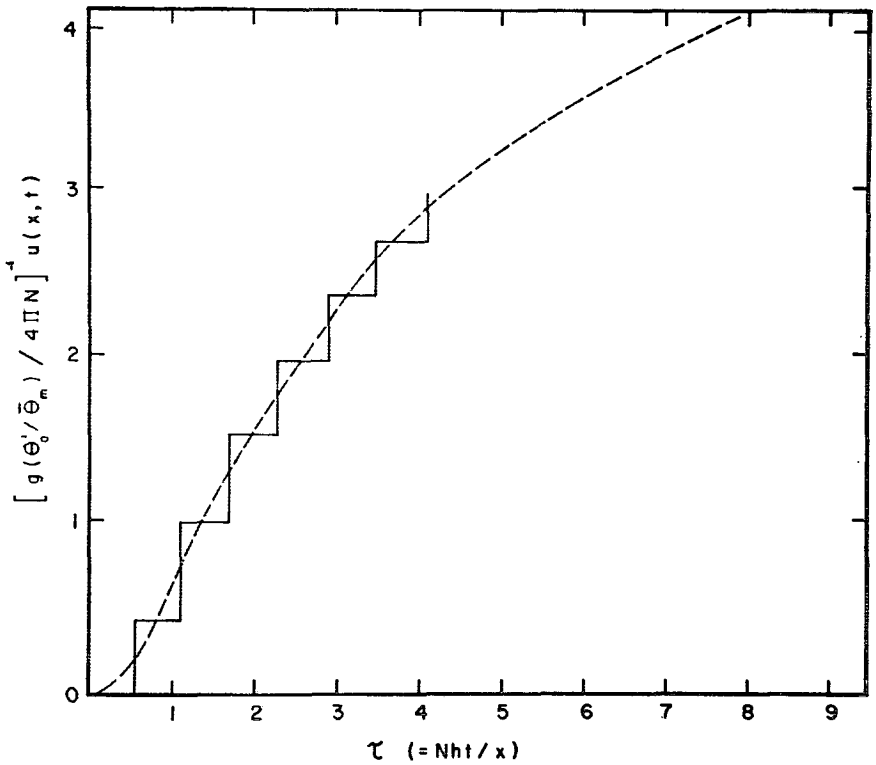

FIG. 8. The wind in the lower layer in Model II calculated when the rigid lid is imposed at a finite height $D=6h$ is given by the full line. This is compared here with the continuous Model II solution (broken line).

to generate short-period waves which subsequently propagate away from the coast at a substantial angle to the horizontal, in addition to hydrostatic waves.

The role of the rigid lid in this analysis is to make the normal modes by which the forerunner propagates discrete instead of continuous. When h/D is small but not infinitesimal, the smooth onset described in Fig. 5 should be replaced by a sequence of step functions (Fig. 8) spaced at intervals of time

$$\Delta t = x\Delta(1/c_n) \approx x/ND.$$

This feature should be perceptible in any realistic numerical model with a rigid lid at a finite height D. The particular result illustrated in Fig. 8 is for Model II and has been obtained from accurate solutions of (26) when $D=6h$ and term-by-term evaluation of the summation (17) using (16) and (28) and the first of Eqs. (29). The trend of this solution is seen to be such as to trace out the continuous Model II solution.

If the rigid lid boundary condition $w=0$ at $z=D$ is replaced by (for example) $p'=0$ at $z=D$, the *form* of the eigenfunctions $\bar{\psi}_n$ [Eqs. (18) and (25)] are unaffected, but the *velocities* c_n are changed. In particular, Eqs. (26) and (31) will be different. This will alter the numerical value of the eigenvalues, but for h/D small, the spacing $\Delta(1/c_n)$ between them will not be changed. Thus, the position of the steps in Fig. 8 is dependent upon the precise upper boundary condition chosen, but the trend of the solution is not. However, in one respect the rigid lid is physically important. Immediately after the insertion of the thermal contrast in the lower layer, the temperature above $z=h$ is still horizontally uniform. The return flow is then driven by a small pressure gradient along the lid. If the lid could not support a pressure perturbation there would inevitably be significant vertical accelerations through it, the vertical scale of the motion would be undefined, and the use of the hydrostatic approximation could not be justified. As vertical displacements develop, however, the return flow takes place at lower levels and the pressure perturbations are predominantly supported by buoyancy forces. The vertical scale is then well-defined and much less than the horizontal scale, and the hydrostatic approximation is valid independently of the lid.

If the heating θ_0' is inserted into a layer of given depth h gradually rather than suddenly, the theory is easily modified. The velocity at a given point $u(x,z,t)$ must be replaced by the smeared value $\int u(x, z, t-t')f(t')dt'$, where $f(t')$ is the distribution function of the rate of heating. The onset of the forerunner is thus more gradual, although for sufficiently large values of x the effect will not be noticeable.

In Models II and III, the circulation does not depend on θ_0', being independent of height throughout the lower

layer. Only an *effective thermal contrast* $\langle\theta_0'\rangle$ defined by

$$\langle\theta_0'\rangle=\frac{2}{h^2}\int_0^h z\theta_0'(z)dz \tag{59}$$

actually enters the theory. This follows from the definition of A_n in (12) and the fact that the $\bar{\psi}_n$ in the lower layer are linear functions of z. When we consider what values of $\langle\theta_0'\rangle$ and h are reasonable for insertion into this theory, it is important to remember that, in fact, the height range through which solar heating is distributed over land increases steadily from sunrise until midafternoon (e.g. Lettau, 1957, Fig. 7.3.5). A possible model of this process is to assume that shortly after dawn the atmosphere is stably stratified with uniform lapse rate $\partial\bar{\theta}/\partial z$ and thereafter a well mixed layer of depth $h(t)$ in which $\theta'=(h-z)(\partial\bar{\theta}/\partial z)$ begins to extend upward. If the rate of supply of heat is constant, then

$$\int_0^h \theta' dz=\frac{h^2}{2}\frac{\partial\bar{\theta}}{\partial z}$$

increases linearly with time; that is, $h\propto t^{\frac{1}{2}}$. Simultaneously, the effective thermal contrast

$$\langle\theta_0'\rangle=\frac{2}{h^2}\frac{\partial\bar{\theta}}{\partial z}\int_0^h z(h-z)dz=\frac{1}{3}\frac{h\partial\bar{\theta}}{\partial z} \tag{60}$$

also increases.

It is therefore difficult to determine the most appropriate hour of the day to take as the moment of starting, if the predictions of Models II or III are to be compared with the real atmosphere. The effects of the depth h of the lower well-mixed layer being time dependent cannot be easily assessed. However, it is clear that gravity waves generated early in the day have a small height scale h and propagate rather slowly, at a rate proportional to h. The circulation is then relatively weak, since total momentum generated per unit time in the lower layer is proportional to h^3. Thus, it seems plausible that any forerunner observed at moderate distances inland would have been generated near or somewhat before the time that the depth of the heated layer attains its diurnal maximum. In the data summarized by Lettau (*loc. cit.*) an adiabatic layer extends upward to 1 km by 1600 local time. From this data we take the effective starting time as 1400, $h=1$ km, and $\partial\bar{\theta}/\partial z=6$C km^{-1}. Then from (60), $\langle\theta_0'\rangle=2$C. Since it is the thermal contrast between far inland and far out to sea that matters, the nocturnal inversion present in the data has been ignored in assigning the dawn thermal structure $\partial\bar{\theta}/\partial z$.

On these considerations, the physical situation at the starting time is that of a well-mixed lower layer extending to 1 km on land and an effective thermal contrast of 2C. However, the thermal structure in the lower layer over the sea is here different from that over land, an effect which cannot be inserted into the forerunner theory. Presumably, the main consequence is that the forerunner propagates at different rates over land and sea. It should be recognized that these estimates are subject to considerable uncertainty and clearly should be dependent on the synoptic situation. For example, the onset of cumulus convection in the morning could take place rather rapidly, establishing a sudden thermal contrast then. The differential release of latent heat signified by the presence of cumulus clouds inland but not over the sea is another factor to be considered in assessing the thermal contrast and the depth through which it is distributed. Thus, the predictions of this theory should not be taken literally. Their main function is to serve as a standard of comparison for more sophisticated numerical models.

Finally, we remark on the omission of a synoptic-scale wind and of the earth's rotation. This step was taken primarily for simplicity, as their effects are known to be important. The former is relatively easily inserted into the analysis. For any of the models in Section 4, a mean wind U would result in the whole flow pattern translating without distortion at speed U. With an offshore wind the development of the forerunner at a given point x would proceed only as far as the stage $\tau=Nh/U$. With an onshore wind the temperature discontinuity itself would be advected inland at speed U. The primary effect of rotation is to cause an acceleration parallel to the coast, proportional to the wind velocity in the forerunner. This shift in wind direction takes roughly $\frac{1}{4}$ pendulum day ≈ 5 hr to become substantial. On a longer time scale still (≈ 10 hr) the inflow is halted by the Coriolis force.

8. Conclusions

Differential heating across a coastline leads to a disturbance there which subsequently grows in the lateral direction, both inland and out to sea. In the vicinity of the growing extremities, the disturbance may be treated with a linearized theory and can be described as the sea-breeze forerunner. Its development at any point may be interpreted as the successive arrival of internal gravity waves propagating away from the coast with the appropriate group velocity. Elsewhere, the disturbance can be treated only by a nonlinear theory and may be formally classified as the sea-breeze circulation.

The structure of the forerunner depends upon the large-scale field of stratification. This has been detailed here for the case when the temperature contrast is switched on through some height range at an initial time. Comparison of results obtained on this theory with observations in the atmosphere is difficult, because the initial time cannot be specified precisely when the depth of the heated layer varies systematically with time through the day.

It seems best to accept the detailed theoretical predictions in this paper only as a guide to interpret the

behavior of a nonlinear numerical model, where the introduction of a realistic thermal forcing presents no special difficulties. The momentum balance argument advanced here should also apply in the nonlinear case and can thus serve as a check on the results of a more general numerical model. Finally, it has been shown that a rigid lid at a finite height is a suitable upper boundary condition to be used in such a model. The effects which are introduced by this choice of upper boundary condition have been identified.

Acknowledgments. This research was supported by the National Science Foundation under grant N7480R.

REFERENCES

Bretherton, F. P., 1967: The time-dependent motion due to a cylinder moving in an unbounded rotating or stratified fluid. *J. Fluid Mech.*, **28**, 545–570.

Estoque, M. A., 1961: A theoretical investigation of the sea breeze. *Quart. J. Roy. Meteor. Soc.*, **87**, 136–146.

——, 1962: The sea breeze as a function of the prevailing synoptic situation. *J. Atmos. Sci.*, **19**, 244–250.

Fisher, E. L., 1961: A theoretical study of the sea breeze. *J. Meteor.*, **18**, 216–233.

Haurwitz, B., 1959: A linear sea breeze model. Quart. Prog. Rept. No. 3, Project Nr 3-36-05-401, New York University College of Engineering, 33 pp.

Lettau, H. H., 1957: *Exploring the Earth's First Mile*, Vol. 1. London, Pergamon Press.

Pearce, E. P., 1955: The calculation of a sea-breeze circulation in terms of the differential heating across the coastline. *Quart. J. Roy. Meteor Soc.*, **81**, 351–381.

Sawyer, J. S., 1959: The introduction of the effects of topography into methods of numerical forecasting. *Quart. J. Roy. Meteor. Soc.*, **85**, 31–43.

Schroeder, M. J., M. A. Fosberg, O. P. Cramer and C. A. O'Dell, 1967: Marine air invasion of the Pacific coast: A problem analysis. *Bull Amer. Meteor. Soc.*, **48**, 802–808.